A single pair of pharyngeal neurons functions as a commander to reject high salt in *Drosophila melanogaster*

Jiun Sang[1,3], Subash Dhakal[1,3], Bhanu Shrestha[1], Dharmendra Kumar Nath[1], Yunjung Kim[1], Anindya Ganguly[2], Craig Montell[2,*], and Youngseok Lee[1,4,*]

[1]Department of Bio and Fermentation Convergence Technology, Kookmin University, Seoul, 02707, Republic of Korea

[2]Neuroscience Research Institute and Department of Molecular, Cellular and Developmental Biology, University of California, Santa Barbara, Santa Barbara, CA United States

[3]These authors contributed equally

[4]Lead Contract

[*]correspondence email, cmontell@ucsb.edu; or ylee@kookmin.ac.kr

ORCID ID: CM, 0000 0001 5637 1482; YL, 0000 0003 0459 1138

Abstract

Salt is a crucial for survival, while excessive NaCl can be detrimental. In the fruit fly, *Drosophila melanogaster*, an internal taste organ, the pharynx, is a critical gatekeeper impacting the decision to accept or reject a food. Currently, our understanding of the mechanism through which pharyngeal gustatory receptor neurons (GRNs) sense high salt are rudimentary. Here, we found that a member of the ionotropic receptor family, IR60b, is exclusively expressed in a pair of GRNs activated by high salt. Using a two-way choice assay (DrosoX) to measure ingestion, we demonstrate that IR60b and two coreceptors IR25a and IR76b, are required to prevent high salt consumption. Mutants lacking external taste organs but retaining the pharynx exhibit much higher salt avoidance than flies with all taste organs but missing the three IRs. Our findings highlight the critical role for IRs in a pair of pharyngeal GRNs to control ingestion of high salt.

36 # Introduction

37 The sense of taste enables animals to find nutritious food while avoiding potentially
38 harmful substances in their environment. Most animals have evolved sophisticated
39 systems to detect and steer clear of consuming levels of substances that are toxic.
40 Salts such as NaCl are vital for a wide array of physiological functions. However,
41 consuming excessive salt can contribute to various health issues in mammals,
42 including hypertension, osteoporosis, gastrointestinal cancer, and autoimmune
43 diseases [1-6]. Therefore, high concentrations of salt are rejected by most animals.

44 Multiple studies have delved into how Na^+ is sensed in the *Drosophila* taste
45 system, shedding light on the mechanisms behind the attraction to low salt and
46 aversion to high salt [7-14]. The major taste organs in flies, are two bilaterally
47 symmetrical labella, each of which is decorated with 31 gustatory hairs (sensilla).
48 These sensilla are characterized based on size (small, S; intermediate, I; large, L).
49 The I-type sensilla harbor either two gustatory receptor neurons (GRNs), while the S-
50 and L-sensilla contain four. These GRNs fall into five classes (A-E) based on their
51 response profiles. These include A GRNs (formerly sugar GRNs), which respond to
52 attractive compounds such as low salt, sugars, glycerol, fatty acids and carboxylic
53 acids, B GRNs (formerly bitter GRNs), which are activated by high Na^+, bitter
54 compounds, acids, polyamines, tryptophan, and L-canavanine, 'C' GRNs respond to
55 water, 'D' GRNs detect high levels of cations such as Na^+, K^+ and Ca^{2+}, and 'E'
56 GRNs sense low Na^+ levels [15].

57 Several of the 66 member ionotropic receptor (IR) family function in the

58 sensation of low and high salt. These include IR76b and Ir25a, which are IR-
59 coreceptors, and therefore have broad roles in sensing many taste stimuli including
60 low and high salt (sodium) [8,12,16], calcium [17], several carboxylic acids [18-20], fatty acids
61 [16,21-23], amino acids [24], and carbonation [25]. A subset of A GRNs, as well as
62 glutamatergic E GRNs are responsible for sensing low salt[8,11,12,15], and this sensation
63 depends on IR56b working together with the broadly tuned IR25a and IR76b [8].
64 Conversely, detection of high salt depends on B GRNs and D GRNs, and IR7c, in
65 conjunction with IR25a and IR76b [7]. Additionally, two Pickpocket channels, PPK11,
66 PPK19, and Sano have been associated with high salt aversion[26,27]. *ppk19* and
67 *ppk11*, which are members of the pickpocket (*ppk*) gene family, are expressed in
68 taste-sensing terminal organs and play a role in appetitive and aversive behavior in
69 response to low and high salt concentrations, respectively [27].

70 In addition to the labellum and taste hairs on other external structures, fruit
71 flies are endowed with an internal organ in the proboscis, called the pharynx, which
72 functions in the decision to keep feeding or reject a food [28-32]. The pharynx includes
73 three separate taste organs that line the esophagous: the labral sense organ (LSO),
74 the ventral cibarial sense organ (VCSO), and the dorsal cibarial sense organ (DCSO)
75 [28,30,31]. Each of these organs include hairless sensilla that house GRNs. A pair of
76 GRNs in the LSO express a member of the gustatory receptor family, *Gr2a*, and
77 knockdown of *Gr2a* in these GRNs impairs the avoidance to slightly aversive levels
78 of Na^+ [14]. Pharyngeal GRNs also promote the aversion to bitter tastants, Cu^{2+}, L-
79 canavanine, and bacterial lipopolysaccharides [33-36]. Other pharyngeal GRNs are
80 stimulated by sugars and contribute to sugar consumption [28,32,37]. Remarkably, two

81 pharyngeal GRNs function in the rejection rather the acceptance of sucrose [38].

82 In this work, we investigated whether IRs function in the pharynx for
83 avoidance of high Na^{+}. We found that IR60b, along with co-receptors IR25a and
84 IR76b are required in the pharynx for preventing high salt consumption. IR60b is
85 exclusively expressed in a pair of pharyngeal GRNs in the LSO, and these neurons
86 are specifically activated by salt but not by any tested bitter compounds. When we
87 optogenetically activated these IR60b-positive GRNs, proboscis extension
88 responses were inhibited, indicating that these GRNs promote aversive behavior.
89 Moreover, introduction of rat TRPV1 into the IR60b neurons induces aversive
90 towards capsaicin, implying that these IR60b-positive GRNs are essential for
91 instinctive avoidance. To validate the findings, we used a two-way choice DrosoX
92 assay to measure actual ingestion levels. We found that the three *Ir* mutants
93 consumed high salt at levels similar to sucrose over an extended period,
94 emphasizing the critical role of this single pair of pharyngeal GRNs in controlling
95 harmful ingestion of high salt.

96

97 # Results and discussion

98 ### *Ir60b* functions in the repulsion to high salt

99 To identify potential salt sensors in *Drosophila melanogaster*, we conducted binary
100 food choice assays using 30 *Ir* mutants (Figures 1A and S1A). Through screens in
101 which we gave the flies a choice between 2 mM sucrose alone or 2 mM sucrose plus
102 a low, attractive level of salt (50 mM NaCl), we confirmed that *Ir76b* [12], *Ir25a*, and

103 *Ir56b* [8], are essential for detecting low salt (Figure S1A). Moreover, consistent with
104 Dweck et al. [8], using tip recordings to assay tastant-induced action potentials, we
105 found that loss of *Ir56b* nearly eliminated spikes in response to low salt (Figure S1B).
106 Using a *Ir56b-GAL4* to drive *UAS-mCD8*::*GFP,* we also confirmed that the reporter
107 was restricted to a subset of A GRNs, which were marked tdTomato (Figures S1D—
108 S1F). We generated a *UAS-Ir56b* transgene which restored normal frequencies of
109 action potentials in *Ir56b*-expressing GRNs (Figure S1B). Moreover, ectopic
110 expression of *UAS-Ir56b* in GRNs that typically have minimal responses to low salt,
111 caused a large increase in salt-induced action potentials (Figure S1C).

112 In our behavioral screen for *Ir* mutants required for avoiding high salt (300
113 mM NaCl), we found that in addition to *Ir7c*, *Ir25a*, and *Ir76b* as previously described
114 [7], *Ir60b* was also required (Figure 1A). The *Ir60b* mutant, $Ir60b^{3}$, was generated by
115 removing 768 base pairs, which spanned from 44 base pairs upstream of the
116 predicted transcription start site to encompass the coding region for the initial 241
117 residues of the 577-amino acid protein (Figure S2A-C). Additionally, we verified the
118 impairment in high salt avoidance using $Ir60b^{1}$, a gene previously investigated by
119 Joseph et al. (Figure S2D) [38]. We conducted dose-response behavioral assays using
120 *Ir60b* mutants, as well as *Ir25a*, *Ir76b* and *Ir7c* and found that all four mutants
121 exhibited significant deficiencies in avoiding salt concentrations ranging from 200
122 mM to 500 mM (Figure 1B). Nevertheless, all of the mutants exhibited a strong
123 aversion to extremely high salt concentrations, reaching 1000 mM, a level twice as
124 concentrated as that found in the ocean. This extreme condition could potentially
125 trigger the activation of additional pain or alarm neurons, serving as a protective

126 mechanism to prevent potential tissue and organ damage.

127

128 **Activation of *Ir60b* neurons inhibits motivation to feed**

129 To investigate whether activation of *Ir60b* neurons induces aversive behavior, we
130 used both chemogenetic and optogenetic approaches. Capsaicin, a ligand for the
131 mammalian TRPV1 channel, does not normally elicit responses in flies (Figure 1C) [39].
132 Therefore, we expressed *UAS-trpV1* under the control of the *Ir60b-GAL4*, and
133 presented the flies with a choice between a 2 mM sucrose and a 2 mM sucrose
134 containing 100 mM capsaicin. We found that the transgenic flies actively avoided
135 capsaicin (Figure 1C), whereas expression of TRPV1 in A (sweet) GRNs (*Gr64f-*
136 *GAL4* and *UAS-trpV1*) induced a preference for capsaicin (Figure 1C). These
137 findings support the idea that the activation of *Ir60b* neurons leads to gustatory
138 avoidance.

139 To further test the proposal that *Ir60b*-positive GRNs elicit aversive behavior,
140 we expressed CsChrimson, a light-activated cation channel[40] in *Ir60b* neurons. As
141 controls we drove *UAS-CsChrimson* either in A GRNs (*Gr5a-GAL4*) or B GRNs
142 (*Gr66a-GAL4*). Upon stimulation with red lights and sucrose, nearly all of the control
143 flies (*UAS-CsChrimson* only) or flies expressing *UAS-CsChrimson* in A GRNs
144 extended their proboscis (Figure 2B). In contrast, the PER was notably diminished in
145 flies expressing *UAS-CsChrimson* in B GRNs (*Gr66a-GAL4*) or in *Ir60b* neurons
146 (*Gr66a-GAL4*; 56.7±4.2% and *Ir60b-GAL4*; 55.0±5.0%, respectively; Figure 1D).
147 These results provide compelling evidence supporting the notion that *Ir60b*-positive
148 GRNs induce behavioral aversion.

149

150 ***Ir60b* is not required in the labellum to sense high salt**

151 To investigate the physiological responses of labellar sensilla to high salt (300 mM),
152 we conducted tip recordings on each of the 31 sensilla (Figure 2A). Five sensilla,
153 including three S-type (S4, S6, and S8) and two L-type (L4 and L6), exhibited the
154 strongest responses to high salt (Figure S3A). These responses were largely
155 dependent on the broadly tuned IR25a and IR76b, as well as *Ir7c* (Figures 2B, 2C
156 and S3B) as reported[7]. Interestingly, the *Ir60b*^{3} deletion mutant did not affect the
157 neuronal responses to high salt in external sensory organs (Figures 2B and 2C). We
158 inactivated individual GRNs by expressing the inwardly rectifying K^+ channel (*UAS-*
159 *Kir2.1*) [41] in A GRNs (*Gr64f-GAL4*) [42], B GRNs (*Gr66a-GAL4*) [43], C GRNs (*ppk28-*
160 *GAL4*) [44], and D GRNs (*ppk23-GAL4*) [17], and confirmed that the aversive behavior
161 and neuronal responses to high salt primarily relied on B and D GRNs (Figures 2D
162 and 2E) as described [11].

163 To examine the gustatory repulsion to high salt that is mediated through the
164 labellum, we conducted proboscis extension response (PER) assays by stimulating
165 the labellum. Starved control and *Ir* mutant flies extend their proboscis when the
166 labellum is lightly touched by a 100 mM sucrose probe (Figure 2F). Upon a second
167 sucrose offering, the various fly lines exhibited slightly and similarly diminished
168 responses (Figure 2H). When we added 300 mM salt to the sucrose, it significantly
169 reduced the PER in the control group (Figures 2G and 2I; first offering 40.9 ± 4.0%;
170 second offering 41.5 ± 3.7%). Both the *Ir25a*^{2} and *Ir76b*^{1} mutants also exhibited
171 suppressed PERs, but the suppression was not as great as in the control (Figures

172 2G and 2I). In contrast, high salt reduced the PER by the *Ir60b*^{3} mutant to a similar
173 extent as the control (Figures 2G and 2I; first offering 41.6 ± 6.5%; second offering
174 47.7 ± 6.7%). This indicates that the labellum of the *Ir60b*^{3} detects 300 mM salt
175 normally, even though the mutant is impaired in avoiding high salt in a two-way
176 choice assay (Figure 1A).

177

178 **High salt sensor in the pharynx**

179 The observations that *Ir60b* is required for the normal aversion to high salt, but does
180 not appear to function in labellar hairs raises the possibility that *Ir60b* is required in
181 the pharynx for salt repulsion. *Ir60b* is expressed in the pharynx where it plays a role
182 in limiting sucrose consumption [38]. *Gr2a* is also expressed in the proboscis and
183 contributes to the repulsion to moderate salt levels (150 mM) [14]. However, the
184 *Gr2a*^{GAL4} mutant displays a normal response to high salt (450 mM) [14]. In our two-way
185 choice assay, which focuses on 300 mM NaCl, we found that salt repulsion displayed
186 by the *Gr2a*^{GAL4} mutant was also indistinguishable from the control (Figure S4).

187 To investigate a role for the pharynx in high salt (300 mM) repulsion, we
188 conducted tests on *Poxn* mutants (*Poxn*$^{70\text{-}28}$/*Poxn*$^{\Delta M22\text{-}B5}$), in which the external
189 chemosensory sensilla have been converted to mechanosensory sensilla [45]. As a
190 result, *Poxn* mutants possess only intact internal gustatory organs. We found that the
191 aversive behavior to high salt was reduced in the *Poxn* mutants relative to the control
192 (Figure 2J). However, the diminished avoidance was significantly different from
193 *Poxn*$^{70\text{-}28}$/*Poxn*$^{\Delta M22\text{-}B5}$;*Ir60b*^{3} mutants, even though *Poxn*$^{70\text{-}28}$/*Poxn*$^{\Delta M22\text{-}B5}$;*Ir60b*^{3}
194 mutants were not significantly different from *Ir60b*^{3} in avoidance to high salt (Figure

195 2J). Furthermore, the *Poxn*$^{70-28}$/*Poxn*$^{\Delta M22-B5}$;*Ir60b*^{3} double mutant exhibited
196 avoidance of high salt at a similar level to *Ir60b*^{3}. This suggests that the internal
197 sensor (IR60b-positive GRNs) can override the activation of the labellum in terms of
198 aversive ingestion of high salt. Subsequently, we hypothesized that IR60b might not
199 act as a primary gustatory sensor but rather as a regulator that allows for continued
200 ingestion.

201

202 **Quantification of reduced high salt ingestion in *Ir60b* mutants**

203 To assess the ingestion of different food types, we employed the binary food choice
204 assay, a qualitative method that utilizes blue, red, or purple dye colors in the
205 abdomen [46]. However, for a more precise quantification of food ingestion, we
206 recently developed the DrosoX system (Figure S5A) [47]. This system allowed us to
207 directly measure the actual amount of food ingested over a period of 6 hours. In
208 these experiments, we present flies with two capillaries: one containing 100 mM
209 sucrose and the other containing 100 mM sucrose mixed with 300 mM NaCl. Control
210 flies exhibited a preference for sucrose-only food, consuming it approximately four
211 times more than the sucrose mixed with salt (Figure 3A). In contrast, the *Ir25a*, *Ir60b*,
212 and *Ir76b* mutants displayed similar total ingestion levels (Figure 3A) and ingestion
213 volume per hour (Figure 3B; ingestion index) for both tastants. In a prior study, it was
214 observed that *Ir60b* mutant flies consumed high salt at a comparable rate to the
215 control group when the total feeding time was recorded [38]. However, the DrosoX
216 system now enables us to precisely quantify the ingestion volume. Additionally, we
217 concurrently assessed two distinct tastants and compared their respective

218 consumption levels. Consequently, our approach for evaluating avoidance behavior
219 differs significantly.

220 To further investigate the requirement for these genes, we performed genetic
221 rescue experiments. We introduced their respective wild-type cDNAs under the
222 control of their cognate *GAL4* drivers, which resulted in a conversion from salt-
223 insensitive behavior to the salt-sensitive behavior observed in wild-type flies (Figures
224 3C-3H). In addition, the defects in the *Ir25a*^{2} and *Ir76b*^{1} mutants were fully rescued
225 by expressing the wild-type *Ir25a* and *Ir76b* transgenes, respectively, in the pharynx
226 using the *Ir60b-GAL4* (Figure 3I-3L). This suggests that both IR25a and IR76b act as
227 coreceptors in the IR60b-expressing GRNs. Furthermore, we investigated whether
228 the expression of *UAS-Ir60b* driven by *Ir25a-GAL4* or *Ir76b-GAL4* could rescue the
229 defects observed in *Ir60b*^{3}. Remarkably, despite the broad expression of IR60b using
230 these *GAL4* drivers, the *Ir60b* salt ingestion defect was eliminated (Figures 3M and
231 3N). Thus, it appears that simultaneous activation of GRNs that elicit attractive and
232 aversive salt responses lead to repulsion. This suggests that activation of GRNs that
233 induce salt aversion may suppress GRNs that function in salt attraction. If so, this
234 would be reminiscent of bitter GRNs that suppress sugar GRNs through a
235 GABAergic mechanism [48].

236 Next, we addressed whether IR60b is specifically required for regulating the
237 ingestion high salt. To investigate this, we assessed the consumption of caffeine,
238 strychnine, and coumarin in *Ir60b*^{3} flies. We found that *Ir60b*^{3} displayed similar
239 consumption patterns to the wild-type control flies for these bitter compounds
240 (Figures 3O, 3P, S5B—S5E). This is in contrast to the impairments exhibited by the

241 *Gr66a*^{ex83} mutant (Figures 3O, 3P, S5B—S5E), which is widely required for sensing
242 many bitter chemicals. This indicates that IR60b is involved in regulating the
243 avoidance of high salt ingestion rather than general avoidance responses to toxic
244 compounds. Nevertheless, the role of IR60b in suppressing feeding is not limited to
245 high salt, since IR60b also functions in the pharynx in inhibiting the consumption of
246 sucrose [38].

247

248 **A single neuron in the LSO depends on *Ir25a*, *IR60b* and *Ir76b* for responding**
249 **to both high salt and sucrose**

250 In addition to IR60b, two other broadly required IRs (IR25a and IR76b) also function
251 in repulsion to high salt. Moreover, we found that we could rescue the *Ir25a*, *Ir60b* or
252 *Ir76b* DrosoX phenotypes using the same *Ir60b-GAL4* to drive expression of the
253 cognate wild-type transgenes in the corresponding mutant backgrounds. These
254 finding imply that all three *Ir*s are coexpressed in the pharynx. Therefore, we
255 examined the relative expression patterns of the *Ir60b-GAL4* reporter with *Ir25a* and
256 *Ir76b* in the pharynx. We observed that the *Ir76b-QF* reporter was expressed in two
257 cells within the labral sensory organ (LSO), one of which colocalized with *Ir60b-*
258 *GAL4* expression (Figure 4A). Additionally, the expression pattern of *Ir25a-GAL4*
259 perfectly overlapped with that of *Ir76b-QF* in the LSO (Figure 4B). Thus, we suggest
260 that *Ir25a*, *Ir60b* and *Ir76b* function in the same GRN in the LSO to limit consumption
261 of high salt. We attempted to induce salt activation in the I-type sensilla by
262 ectopically expressing *Ir60b*, similar to what was observed with *Ir56b* [8]; however, this
263 did not generate a salt receptor (Figures S6A). Thus, the IR25a/IR60a/IR76b

264 channel may require an additional subunit.

265 To determine whether this GRN in the LSO is activated by high salt, we
266 examined Ca^{2+} responses in the LSO using *UAS-GCaMP6f*, expressed under the
267 control of each *GAL4* driver. In the wild-type LSO, we identified a single cell that
268 responded to 300 mM NaCl (Figure 4C). These data show that the single GRN in the
269 LSO that expresses all three reporters responds to high salt. Moreover, this neuron
270 responded robustly to 300 mM to 1000 mM Na^+ but not to a low level of Na^+ (50 mM;
271 Figure 4E). We then examined the Ca^{2+} responses in the *Ir25a*^{2}, *Ir60b*^{3}, and *Ir76b*^{1}
272 mutants, and found that each of them failed to respond to NaCl (Figures 4D and 4E).
273 Additionally, we rescued the deficits in the GCaMP6f responses exhibited by each
274 mutant by expressing a wild-type transgene under control of the corresponding
275 GAL4 driver (Figure 4F). We also tested other Cl^- salts ($CaCl_2$, $MgCl_2$, and KCl) to
276 determine if Cl^- rather an Na^+ induced responses in the IR60b neuron. However,
277 none of these other salts affected these neurons at 50 mM, 300 mM, and 500 mM
278 concentrations tested (Figure 4G). In contrast, NaBr induced GCaMP6f responses
279 (Figure 4H). Thus, the *Ir60b* neuron is responsive to Na^+ and not Cl^-. Due to the
280 effects of NaBr on the *Ir60b* neuron, we used the DrosoX assay to determine
281 whether 300 mM NaBr suppressed ingestion of sucrose. We found that the impact of
282 NaBr on sucrose ingestion was similar to that with NaCl (Figures S6B and S6C). We
283 also found that bitter compounds such as quinine, caffeine, strychnine, lobeline,
284 denatonium, and coumarin could not activate *Ir60b* neurons at the concentrations of
285 5 mM and 50 mM tested (Figure 4I).

286 It has been shown previously that *Ir60b* is required in single neuron in the
287 pharynx for suppressing sucrose feeding, and this neuron responds to sucrose. [38]

288 Therefore, we tested whether the same neuron in the LSO that responds to salt also
289 responds to sucrose. Using GCaMP6f, we found that the *Ir60b* neuron was activated
290 by sucrose in the LSO of control flies, but not in the *Ir25a*, *Ir60b* and *Ir76b* mutants
291 (Figure 4J). Thus, we conclude that the same LSO neuron depends on the presence
292 of the same three receptors (IR25a, IR60b, and IR76b) for suppressing feeding in
293 response to high salt or to sucrose. Mcdowell et al. demonstrated the presence of
294 IR7c in labellar GRNs sensitive to high salt. They also unveiled the collaborative role
295 of IR7c with IR25a and IR76b in perceiving and responding to high salt
296 concentrations. Consequently, we investigated whether IR7c played a potential role
297 in *Ir60b*-positive pharyngeal GRNs. However, our experiments did not reveal any
298 physiological defects in *Ir7c* mutant flies (Figure S7A). Furthermore, our findings
299 indicated that *Ir7c* is not expressed within the *Ir60b*-positive GRNs (Figure S7B—D).
300 Although prior research had identified the involvement of IR7c, IR25a, and
301 IR76b in the labellar GRNs for high salt detection, our study introduces a perspective
302 by highlighting the combination of IR25a, IR60b, and IR76b as internal molecular
303 sensors responsible for detecting and ingesting high salt.
304
305

306 # Materials and methods

307 ## Key resources table

Reagent type	Designation	SOURCE	IDENTIFIER
Antibody	Mouse anti-GFP	Molecular probes	Cat # A11120; RPID: AB_221568
Antibody	Rabbit anti-DsRed	Clontech	Cat # 632496; RPID: AB_10013483
Antibody	Goat Anti-mouse Alexa Fluro 488	Invitrogen	Cat # A32723; RRID: AB_2633275
Antibody	Goat anti-rabbit Alexa Fluor 568	Invitrogen	Cat # A11011; RPID: AB_143157
Chemical compound, drug	Sucrose	Sigma-Aldrich	Cat # 9378S
Chemical compound, drug	Tricholine citrate	Sigma-Aldrich	Cat # T0252
Chemical compound, drug	Sulforhodamine B	Sigma-Aldrich	Cat # 230162
Chemical compound, drug	Capsaicin	Sigma-Aldrich	Cat # M2028
Chemical compound, drug	Caffeine	Sigma-Aldrich	Cat # C02750
Chemical compound, drug	$CaCl_2$ dihydrate	Sigma-Aldrich	Cat # C3881
Chemical compound, drug	KCl	Sigma-Aldrich	Cat # P9541
Chemical compound, drug	Quinine	Sigma-Aldrich	Cat # Q1125
Chemical compound, drug	Strychnine	Sigma-Aldrich	Cat # S8753
Chemical compound, drug	Lobeline	Sigma-Aldrich	Cat # 141879
Chemical compound, drug	Denatonium	Sigma-Aldrich	Cat # D5765
Chemical compound, drug	Coumarin	Sigma-Aldrich	Cat # C4261
Chemical compound, drug	Brilliant blue FCF	Wako Pure Chemical Industry	Cat # 027-12842
Chemical compound, drug	Paraformaldehyde	Electron Microscopy Sciences	Cat # 15710

Chemical compound, drug	NaCl	LPS solution	Cat # NACL01
Chemical compound, drug	$MgCl_2$ hexahydrate	SAMCHUN	Cat # M0038
Chemical compound, drug	NaBr	DUKSAN	Cat # S2531
Chemical compound, drug	Goat Serum, New Zealand origin	Gibco	Cat # 16210064
Genetic reagent (*Drosophila melanogaster*)	w^{1118}	Bloomington *Drosophila* Stock Center	BDSC:5905
Genetic reagent (*Drosophila melanogaster*)	$Ir7a^{1}$	Dr. Y. Lee	[20]
Genetic reagent (*Drosophila melanogaster*)	$Ir7g^{1}$: $y^{1}w^{*}Mi\{y^{+mDint2}=MIC\}Ir7g^{MI06687}$	Bloomington *Drosophila* Stock Center	BDSC:42420
Genetic reagent (*Drosophila melanogaster*)	$IR7c^{GAL4}$	Dr. M. D. Gordon	[7]
Genetic reagent (*Drosophila melanogaster*)	$Ir8a^{1}$: $w^{*}TI\{w[+m^{*}]=TI\}Ir8a^{1};Bl^{1}L^{2}/CyO$	Bloomington *Drosophila* Stock Center	BDSC:23842
Genetic reagent (*Drosophila melanogaster*)	$Ir10a^{1}$: $w^{1118}Mi\{GFP^{E.3xP3}=ET1\}Ir10a^{MB03273}$	Bloomington *Drosophila* Stock Center	BDSC:41744
Genetic reagent (*Drosophila melanogaster*)	$Ir21a^{1}$: $w^{1118};PBac\{w^{+mC}=PB\}Ir21a^{c02720}$	Bloomington *Drosophila* Stock Center	BDSC:*10975*
Genetic reagent (*Drosophila melanogaster*)	$Ir25a^{2}$	Dr. L. Voshall	[49]
Genetic reagent (*Drosophila melanogaster*)	$Ir47a^{1}$	Dr. Y. Lee	[20]
Genetic reagent (*Drosophila melanogaster*)	$Ir48a^{1}$: $w^{1118};Mi\{GFP^{E.3xP3}=ET1\}Ir48a^{MB09217}$	Bloomington *Drosophila* Stock Center	BDSC:26453
Genetic reagent (*Drosophila melanogaster*)	$Ir48b^{1}$: $w^{1118};Mi\{GFP^{E.3xP3}=ET1\}Ir48b^{MB02315}$	Bloomington *Drosophila* Stock Center	BDSC:23473
Genetic reagent (*Drosophila melanogaster*)	$Ir51b^{1}$: $w^{1118};PBac\{w^{+mC}=PB\}row^{c00387}$ $Ir51b^{c00387}$	Bloomington *Drosophila* Stock Center	BDSC:10046
Genetic reagent (*Drosophila melanogaster*)	$Ir52a^{1}$	Dr. Y. Lee	[20]
Genetic reagent (*Drosophila melanogaster*)	$Ir52b^{1}$: $w^{1118};Mi\{GFP^{E.3xP3}=ET1\}Ir52b^{MB02231}$ /SM6a	Bloomington *Drosophila* Stock Center	BDSC:25212
Genetic reagent (*Drosophila melanogaster*)	$Ir52c^{1}$: $w^{1118};Mi\{GFP^{E.3xP3}=ET1\}Ir52c^{MB04402}$	Bloomington *Drosophila* Stock Center	BDSC:24580

Genetic reagent (*Drosophila melanogaster*)	*Ir56a*^{1}	Dr. Y. Lee	[20]
Genetic reagent (*Drosophila melanogaster*)	*Ir56b*^{1}: *w*^{1118};Mi{GFP$^{E.3xP3}$=ET1}Ir56b^{MB09950}	Bloomington *Drosophila* Stock Center	BDSC:27818
Genetic reagent (*Drosophila melanogaster*)	*Ir56d*^{1}: *w*;Ir56d*^{1}	Bloomington *Drosophila* Stock Center	BDSC:81249
Genetic reagent (*Drosophila melanogaster*)	*Ir60b*^{3}	Dr. Y. Lee	In this study
Genetic reagent (*Drosophila melanogaster*)	*Ir62a*^{1}: y^{1}w*;Mi{y$^{+mDint2}$=MIC}Ir62a^{MI00895}Iml1^{MI00895}/TM3, Sb^{1} Ser^{1}	Bloomington *Drosophila* Stock Center	BDSC:32713
Genetic reagent (*Drosophila melanogaster*)	*Ir67a*^{1}: y^{1}w*;Mi{y$^{+mDint2}$=MIC}Ir67a^{MI11288}	Bloomington *Drosophila* Stock Center	BDSC:56583
Genetic reagent (*Drosophila melanogaster*)	*Ir75d*^{1}: *w*^{1118};Mi{GFP$^{E.3xP3}$=ET1}Ir75d^{MB04616}	Bloomington *Drosophila* Stock Center	BDSC:*24205*
Genetic reagent (*Drosophila melanogaster*)	*Ir76b*^{1}	Dr. C. Montell	[12]
Genetic reagent (*Drosophila melanogaster*)	*Ir85a*^{1}: *w*^{1118};Mi{GFP$^{E.3xP3}$=ET1}Ir85a^{MB04613} Pif1A^{MB04613}	Bloomington *Drosophila* Stock Center	BDSC:*24590*
Genetic reagent (*Drosophila melanogaster*)	*Ir92a*^{1}: *w*^{1118};Mi{GFP$^{E.3xP3}$=ET1}Ir92a^{MB03705}	Bloomington *Drosophila* Stock Center	BDSC:*23638*
Genetic reagent (*Drosophila melanogaster*)	*Ir94a*^{1}	Dr. Y. Lee	[20]
Genetic reagent (*Drosophila melanogaster*)	*Ir94b*^{1}:*w*^{1118};Mi{GFP$^{E.3xP3}$=ET1}Ir94b^{MB02190}	Bloomington *Drosophila* Stock Center	BDSC:*23424*
Genetic reagent (*Drosophila melanogaster*)	*Ir94c*^{1}	Dr. Y. Lee	[20]
Genetic reagent (*Drosophila melanogaster*)	*Ir94d*^{1}:y^{1}w*;Mi{y$^{+mDint2}$=MIC}Ir94d^{MI01659}CG17380^{MI01659}	Bloomington *Drosophila* Stock Center	BDSC:33132
Genetic reagent (*Drosophila melanogaster*)	*Ir94f*^{1}: y^{1}w*;Mi{y$^{+mDint2}$=MIC}Ir94f^{MI00928}	Bloomington *Drosophila* Stock Center	BDSC:33095
Genetic reagent (*Drosophila melanogaster*)	*Ir94g*^{1}: *w*^{1118};Mi{GFP$^{E.3xP3}$=ET1}Ir94g^{MB07445}	Bloomington *Drosophila* Stock Center	BDSC:25551
Genetic reagent (*Drosophila melanogaster*)	*Ir94h*^{1}	Dr. Y. Lee	[20]
Genetic reagent (*Drosophila melanogaster*)	*Ir100a*^{1}: *w*^{1118};P{w^{+mC}=EP}Ir100a^{G19846} CG42233^{G19846}	Bloomington *Drosophila* Stock Center	BDSC:*31853*

Genetic reagent (*Drosophila melanogaster*)	*UAS-mCD8::GFP*	Bloomington Drosophila Stock Center	BDSC:5137
Genetic reagent (*Drosophila melanogaster*)	*UAS-mCD8::GFP*	Bloomington Drosophila Stock Center	BDSC:32184
Genetic reagent (*Drosophila melanogaster*)	*UAS-Kir2.1*	Bloomington *Drosophila* Stock Center	BDSC:*6595*
Genetic reagent (*Drosophila melanogaster*)	*UAS-Ir25a*	Dr. Y. Lee	[17]
Genetic reagent (*Drosophila melanogaster*)	*UAS-Ir60b*	Dr. Y. Lee	In this study
Genetic reagent (*Drosophila melanogaster*)	*UAS-Ir76b*	Dr. C. Montell	[12]
Genetic reagent (*Drosophila melanogaster*)	*Ir25a-GAL4*	Dr. L. Vosshall	[49]
Genetic reagent (*Drosophila melanogaster*)	*Ir60b-GAL4*	Dr. C. Montell	[38]
Genetic reagent (*Drosophila melanogaster*)	*Ir76b-GAL4*	Dr. C. Montell	[12]
Genetic reagent (*Drosophila melanogaster*)	*ppk23-GAL4*	Dr. K. Scott	[50]
Genetic reagent (*Drosophila melanogaster*)	*ppk28-GAL4*	Dr. H. Amrein	[44]
Genetic reagent (*Drosophila melanogaster*)	*Gr66a-GAL4*	Dr. H. Amrein	[43]
Genetic reagent (*Drosophila melanogaster*)	*Gr64f-GAL4*	Dr. A. Dahanukar	[17]
Genetic reagent (*Drosophila melanogaster*)	*Ir76b-QF*	Bloomington *Drosophila* Stock Center	BDSC:51312
Genetic reagent (*Drosophila melanogaster*)	*QUAS-tdTomato*: y^1w^{1118}; P{QUAS-mtdTomato-3xHA}26	Bloomington *Drosophila* Stock Center	BDSC:30005
Genetic reagent (*Drosophila melanogaster*)	$Poxn^{\Delta M22-B5}$: y^1w^{67c23}; Mi{ET1}$Poxn^{MB00113}$	Bloomington *Drosophila* Stock Center	BDSC:22701
Genetic reagent (*Drosophila melanogaster*)	$Poxn^{70-28}$: $Poxn^{70}$/CyO; twi-gal4, UAS-2XEGFP	Bloomington *Drosophila* Stock Center	BDSC:60688
Software	Origin Pro Version	Dr. Y. Lee	https:/www.originlab.com
Software	GraphPad Prism	Dr. Y. Lee	https:/www.graphpd.com

Software	Autospike 3.1 software	Dr. Y. Lee	https://www.syntech.co.za/
Software	Fiji/ImageJ software	Dr. Y. Lee	https://fiji.sc
Software	ZEN lite 2.5 blue	Dr. Y. Lee	https://www.zeiss.com/

308

309 **Generation of *Ir60b*^{3} and *UAS-Ir60b* lines**

310 The *Ir60b*^{3} mutant were generated by ends-out homologous recombination [51]. For
311 generating the construct to injections, approximately two 3-kb genomic fragments
312 were amplified by PCR, and subcloned the DNAs into the pw35 vector of NotI and
313 BamHI sites. Assuming the "A" of the "ATG" starts codon as "+1", the deleted region
314 was -44 to +724. The construct was injected into *w*^{1118} embryos by Best Gene Inc.
315 We outcrossed the mutant with *w*^{1118} for 6 generations.

316 To generate the *UAS-Ir60b* transgenic strain, we employed mRNA to perform
317 reverse transcription polymerase chain reaction (RT-PCR) on the full-length *Ir60b*
318 cDNA, which was subsequently subcloned into the pUAST vector. The insertion took
319 place between the EcoRI and NotI sites designated for *UAS-Ir60b*. The primer set
320 used for amplification is as follows: 5'-GAGAATTCAACTCGAAAATGAGGCGG-3'
321 and
322 5'-ATGCGGCCGCAATGCTAATTTTG-3'. The integrity of the cloned cDNA was
323 verified through DNA sequencing. Subsequently, the transformation vector harboring
324 the respective constructs was introduced into *w*^{1118} embryos via injection (KDRC).

325

326 **Binary food choice assay**

327 We conducted binary food choice assays following the methods outlined in a
328 previous study[46]. Initially, a group of 40–50 flies (3-6 days old) were subjected to an

329 18-hour starvation period on a 1% agarose substrate. Two mixtures were prepared,
330 each containing a specific dye, and they were distributed in a zigzag pattern. The
331 first mixture consisted of 1% agarose, the indicated concentration of saponin, and 5
332 mM sucrose with red dye (sulforhodamine B, 0.1 mg/ml). The second mixture
333 contained 1% agarose, 1 mM sucrose, and blue dye (Brilliant Blue FCF, 0.125
334 mg/ml). The prepared 72-well microtiter dish was then used to transfer the flies,
335 which was placed in a dark and humid chamber. After feeding, the flies were
336 sacrificed by freezing them at -20°C. Subsequently, their abdomen colors were
337 examined under a microscope to identify the presence of red, blue, or purple dye,
338 allowing us to segregate them accordingly. The counts were taken for the number of
339 flies with blue (N_B), red (N_R), and purple (N_P) abdomens. The preference index (P.I)
340 was calculated using the following equation: $(N_B - N_R)/(N_R + N_B + N_P)$ or $(N_R - N_B)/(N_R$
341 $+ N_B + N_P)$, depending on the specific dye/tastant combinations. A P.I. of -1.0 or 1.0
342 indicated a complete preference for either 5 mM sucrose with saponin or 1 mM
343 sucrose alone, respectively. A P.I. of 0.0 indicated no preference between the two
344 food alternatives.
345

346 **Chemical reagent**

347 Sucrose (CAS No. 57-50-1), tricholine citrate (TCC) (CAS No. 546-63-4),
348 sulforhodamine B (CAS No. 3520-42-1), capsaicin (CAS No. 404-86-4), caffeine
349 (CAS No. 58-08-2), $CaCl_2$ dihydrate (CAS No. 10035-04-8), KCl (CAS No. 7447-40-
350 7), quinine (CAS No. 6119-47-7), strychnine (CAS No. 1421-86-9), lobeline (CAS No.
351 134-63-4), denatonium (CAS No. 6234-33-6), and coumarin (CAS No. 91-64-5) were
352 purchased from Sigma-Aldrich (USA). Brilliant blue FCF (CAS No. 3844-45-9) was

353 purchased from Wako Pure Chemical Industry (Japan). Paraformaldehyde (CAS No.
354 30525-89-4) was purchased from Electron Microscopy Sciences (USA). NaCl (CAS
355 No. 7647-14-5) was purchased from LPS solution (Korea). NaBr (CAS No. 7647-15-
356 6) was purchased from DUKSAN (Korea). Goat serum, New Zealand Origin was
357 purchased from Gibco (USA).
358

359 **Droso-X assay**

360 We conducted Droso-X assays following the methods outlined in a previous study[47].
361 The amount of ingestion was measured using a Droso-X system (Scitech Korea,
362 Korea) located in a controlled incubator (25°C, 60% humidity). To quantify the
363 ingestion, a mixture comprising 100 mM sucrose and the specified concentration of
364 chemicals was injected into a glass tube (Cat. No. 53432-706; VWR International,
365 USA) using a syringe (KOVAX-SYRINGE 1 ml 26G; KOREA VACCINE, Korea) and
366 needle (Cat No. 90025; Hamilton, Switzerland). Each cuvette contained flies (3-6
367 days old) and was physically isolated to prevent them from consuming the solution
368 prior to the experiment. The experiment was conducted for a duration of 6 hours,
369 specifically from 9 am to 3 pm. The DROSO X&XD software (Scitech Korea, Korea)
370 was utilized by the Droso-X system to record the amount of solution consumed. The
371 ingestion amount at time X (X h) was calculated as the difference between the initial
372 solution amount (0 h) and the solution amount at time X.
373 The ingestion index (I.I) was calculated in each time point using the following
374 equation: (Ingestion $volume_{DrosoX}$ - Ingestion $volume_{DrosoXD}$)/(Ingestion $volume_{DrosoX}$ +
375 Ingestion $volume_{DrosoXD}$) or (Ingestion $volume_{DrosoXD}$ - Ingestion
376 $volume_{DrosoX}$)/(Ingestion $volume_{DrosoXD}$ + Ingestion $volume_{DrosoX}$), depending on the

377 specific tastant combinations. A I.I. of 0.0 indicated no preference based on their
378 ingestion between the two food alternatives.
379
380 **Electrophysiology**
381 Electrophysiology, specifically the tip recording assay, was conducted following the
382 previously described method[52]. The tip recordings were carried out based on
383 Tanimura's nomenclature. The average frequencies of action potentials (spikes/s)
384 evoked in response are presented, with only spikes occurring between 50 and 550
385 ms included in the count. For the tip recordings, we followed the established protocol
386 using the specified concentration of saponin dissolved in distilled water with 30 mM
387 tricholine citrate (TCC) for the assay. These electrolytes, 1 mM KCl or 30 mM TCC,
388 served as the recording medium. To begin the recordings, we immobilized flies (3-6
389 days old) by exposing them to ice. A reference glass electrode filled with Ringer's
390 solution was inserted through the back thorax and passed into the proboscis. The
391 sensilla on the labial palp were stimulated with a compound dissolved in the buffer
392 solution of the recording pipette, which had a tip diameter of 10-20 μm. The
393 recording electrode was connected to a pre-amplifier (Taste PROBE, Syntech,
394 Germany), which amplified the signals by a factor of 10 using a signal connection
395 interface box (Syntech) and a 100-3,000 Hz band-pass filter. The recorded action
396 potentials were acquired at a sampling rate of 12 kHz and analyzed using Autospike
397 3.1 software (Syntech). Subsequently, recordings were performed on the indicated
398 sensilla on the labial palp.
399
400 **Proboscis extension response assay**

401 The proboscis extension response experiment was conducted with some
402 modifications previously described by a previous study[53]. A group of 20-25 flies (3-6
403 days old) was deprived of food for 18-20 hours in vials containing wet Kimwipe paper
404 with tap water. After briefly anesthetizing the flies on ice, they were carefully trapped
405 inside a pipette tip with a volume of 20-200 µl. To expose their heads, the edge of
406 the pipette tip was gently cut using a paper cutter blade. The protruded head and
407 proboscis were used to deliver stimuli during the experiment. To stimulate the flies'
408 tarsi, the head/proboscis and forelegs were extended outside the pipette tip without
409 causing any harm. To eliminate any potential biases due to thirst, water was initially
410 provided to the flies. For both the positive control and initial stimulation, a 2%
411 sucrose solution was used. The tastant stimuli, consisting of either 2% sucrose or
412 300 mM NaCl, were presented using Kimwipe paper as the medium. To conduct
413 these experiments, we selected flies that responded to sucrose. Flies that did not
414 exhibit a reaction to the sucrose during the initial exposure were excluded from the
415 experiment. The same conditions as the initial exposures were maintained for the
416 second exposure. Each test round involved the use of more than 10 flies.
417

418 **Immunohistochemistry**

419 We performed immunohistochemistry as previously described[54] with slight
420 modifications. The labella of flies (6-8 days old) were dissected and fixed in a
421 solution containing 4% paraformaldehyde (Electron Microscopy Sciences, Cat No
422 15710) and 0.2% Triton X-100 for 15 minutes at room temperature. After that, the
423 tissues were washed three times with PBST (1x PBS and 0.2% Triton X-100) and
424 then bisected using a razor blade. Subsequently, the tissues were incubated in

425 blocking buffer (0.5% goat serum in 1x PBST) for 30 minutes at room temperature.
426 To detect the target protein, primary antibodies (mouse anti-GFP; Molecular Probes,
427 Cat No A11120; diluted 1:1,000) were added to fresh blocking buffer and left to
428 incubate with the labellum samples overnight at 4 °C. Following this, the tissues
429 were washed three times with PBST and incubated with the secondary antibody
430 (goat anti-mouse Alexa Fluor 488, diluted 1:200) for 4 hours at 4 °C. Afterwards, the
431 tissues were washed three times with PBST and placed in 1.25x PDA mounting
432 buffer (containing 37.5% glycerol, 187.5 mM NaCl, and 62.5 mM Tris pH 8.8). Finally,
433 the samples were visualized using a Leica Stellaris 5 confocal microscope.
434

435 ***Ex vivo* calcium imaging**

436 *Ex vivo* Ca^{2+} imaging was performed as previously described[55] with slight
437 modifications. *Ex-vivo* calcium imaging was conducted using a low melting agarose
438 method. For the experimental process, flies (6-8 days old) expressing *UAS-*
439 *GCaMP6f* driven by *Ir25a-GAL4*, *Ir60b-GAL4*, and *Ir76b-GAL4* were used
440 (incubation conditions: humidity: 50-60%, temperature: 25°C, Light/Dark: 12/12
441 hours). A 0.5% low melting agarose solution was prepared and applied to a confocal
442 dish (Cat No. 102350, SPL LIFE SCIENCE, Korea). A mild swallow deep well was
443 prepared for sample fixation. Subsequently, the heads of the flies were carefully
444 decapitated using sharp razor blades, followed by excising a small portion of the
445 labellum in the extended proboscis region to facilitate tastant access to pharyngeal
446 organs. The prepared tissue sample was then carefully fixed in an inverted position
447 in the pre-prepared well. Videos were recorded with Axio Observer 3 (Carl Zeiss)
448 Adult hemolymph (AHL) composites 108 mM NaCl, 5 mM KCl, 8.2 mM $MgCl_2$, 2 mM

449 $CaCl_2$, 4 mM $NaHCO_3$, 1 mM NaH_2PO_4, and 5 mM HEPES pH 7.5. A pre-stimulus
450 solution, AHL was used, followed by the stimulus solution after 60 seconds, enabling
451 direct access of the stimulant with AHL to the pharyngeal neurons. GCaMP6f
452 fluorescence was observed using a fluorescence microscope with a 20x objective,
453 specifically focusing on the relevant area of the pharynx. Videos were recorded at a
454 speed of two frames per second. Neuronal fluorescent activity changes were
455 recorded for 5 minutes following stimulus application. Fiji/ImageJ software
456 (https://fiji.sc) was used to measure fluorescence intensities. A region of interest (ROI)
457 was drawn around the cell bodies, and the Time-Series Analyzer Plugin, developed
458 by Balaji, J. (https://imagej.nih.gov/ij/plugins/time-series.html), was utilized to
459 measure the average intensity for ROIs during each frame. The average pre-
460 stimulation value before chemical stimulation was calculated. ΔF/F (%) was
461 determined using the formula $(F_{max}-F_0)/F_0 \times 100\%$, where F0 represents the baseline
462 value of GCaMP6f averaged for 10 frames immediately before stimulus application,
463 and Fmax is the maximum fluorescence value observed after stimulus delivery.
464

465 ## Statistical analysis

466 The error bars on the graph indicate the standard error of the means (SEMs), while
467 the dots represent the number of trials conducted for the experiment. To compare
468 multiple datasets, we utilized single-factor ANOVA coupled with Scheffe's analysis
469 as a *post hoc* test. Pairwise comparisons were conducted using Student's t-test.
470 Statistical significance is denoted by asterisks (*$p < 0.05$, **$p < 0.01$). We performed
471 all statistical analyses using Origin Pro 8 for Windows (ver. 8.0932; Origin Lab
472 Corporation, USA).

Acknowledgements

This work was supported by grants to Y.L. from the National Research Foundation of Korea (NRF) funded by the Korea government (MIST) (NRF-2021R1A2C1007628) and Biomaterials Specialized Graduate Program through the Korea Environmental Industry and Technology Institute (KEITI) funded by the Ministry of Environment (MOE) and grants to C.M. from the National Institute on Deafness and other Communication Disorders (NIDCD), R01-DC007864 and R01-DC016278. S.D., B.S., and D.N were supported by the Global Scholarship Program for Foreign Graduate Students at Kookmin University in Korea.

Additional information

Funding

Funder	Grant reference number	Author
National Research Foundation of Korea (NRF) funded by the Korea government (MIST)	NRF-2021R1A2C1007628	Youngseok Lee
National Institute on Deafness and other Communication Disorders (NIDCD)	R01-DC007864	Craig Montell
National Institute on Deafness and other Communication Disorders (NIDCD)	R01-DC016278	Craig Montell

Author contributions

J.S. and S.D. performed most of the genetic studies and physiology. J.S. and Y.L. conceived and designed the experiments. B.S. confirmed optogenetics and ectopic experiments. D.N. worked on low salt sensors. Y.K. generated most new reagents and conducted screening for high salt sensor in the initial stage. A.G. worked on the

initial calcium imaging. C.M. and Y.L. supervised the project and wrote the manuscript.

Author ORCIDs

Jiun Sang https://orcid.org/0000-0002-0824-8428

Dhakal Subash https://orcid.org/0000-0002-5380-1130

Bhanu Shrestha https://orcid.org/0000-0002-2945-2305

Dharmendra Kumar Nath https://orcid.org/0000-0001-6105-6970

Yunjung Kim

Anindya Ganguly https://orcid.org/0000-0002-4798-0806

Craig Montell http://orcid.org/0000-0001-5637-1482

Youngseok Lee http://orcid.org/0000-0003-0459-1138

Additional files

Supplementary files

- Supplementary Figures S1-S5

Data availability

Source data for all figures contained in the manuscript and SI have been deposited in 'fiigshare' (https://doi.org/10.6084/m9.figshare.23939394).

Supplementary files

514 • Supplemental figure 1 code for ‘Requirements for three *Ir*s for preferred low salt-
515 containing food’ presented in Figure 1.
516 • Supplemental figure 2 code for ‘Gene structure of *Ir60b* locus, generation of *Ir60b*^{3}
517 and behavioral defect of *Ir60b*^{1} in high salt avoidance in Figure 1.
518 • Supplemental figure 3 code for ‘Electrophysiological responses with high salt’
519 presented in Figure 2.
520 • Supplemental figure 4 code for ‘The preference of *Gr2a* mutant with high salt’
521 presented in Figure 2.
522 • Supplemental figure 5 code for ‘DrosoX system and measurement of food intake
523 using strychnine and coumarin’ presented in Figure 3.
524 • Supplemental figure 6 code for ‘Measurement of food intake of 300 mM NaBr and
525 ectopic experiment of IR60b’ presented in Figure 4.
526 • Supplemental figure 7 code for ‘Quantification of calcium response in *Ir7c* mutants
527 and control groups within the *Ir60b*-positive GRNs, alongside expression profiling of
528 *Ir7c* and *Ir60b*’ presented in Figure 4.

529 # References

530 1. Heaney, R.P. (2006). Role of dietary sodium in osteoporosis. Journal of the
531 American College of Nutrition *25*, 271S-276S.
532 2. Jones, G., Beard, T., Parameswaran, V., Greenaway, T., and Von Witt, R.
533 (1997). A population-based study of the relationship between salt intake, bone
534 resorption and bone mass. European journal of clinical nutrition *51*, 561-565.
535 3. Luft, F., Rankin, L., Bloch, R., Weyman, A., Willis, L., Murray, R., Grim, C., and
536 Weinberger, M. (1979). Cardiovascular and humoral responses to extremes of
537 sodium intake in normal black and white men. Circulation *60*, 697-706.
538 4. Sharif, K., Amital, H., and Shoenfeld, Y. (2018). The role of dietary sodium in
539 autoimmune diseases: The salty truth. Autoimmunity reviews *17*, 1069-1073.
540 5. Strazzullo, P., D′Elia, L., Kandala, N.-B., and Cappuccio, F.P. (2009). Salt
541 intake, stroke, and cardiovascular disease: meta-analysis of prospective
542 studies. Bmj *339*.
543 6. Neal, B., Wu, Y., Feng, X., Zhang, R., Zhang, Y., Shi, J., Zhang, J., Tian, M.,
544 Huang, L., and Li, Z. (2021). Effect of salt substitution on cardiovascular
545 events and death. New England Journal of Medicine *385*, 1067-1077.
546 7. McDowell, S.A., Stanley, M., and Gordon, M.D. (2022). A molecular
547 mechanism for high salt taste in Drosophila. Current Biology *32*, 3070-3081.
548 e3075.
549 8. Dweck, H.K., Talross, G.J., Luo, Y., Ebrahim, S.A., and Carlson, J.R. (2022).
550 Ir56b is an atypical ionotropic receptor that underlies appetitive salt response
551 in Drosophila. Current Biology *32*, 1776-1787. e1774.

552 9. Dey, M., Ganguly, A., and Dahanukar, A. (2023). An inhibitory mechanism for
553 suppressing high salt intake in Drosophila. Chemical Senses *48*, bjad014.
554 10. Lee, M.J., Sung, H.Y., Jo, H., Kim, H.-W., Choi, M.S., Kwon, J.Y., and Kang, K.
555 (2017). Ionotropic receptor 76b is required for gustatory aversion to excessive
556 Na+ in Drosophila. Molecules and cells *40*, 787.
557 11. Jaeger, A.H., Stanley, M., Weiss, Z.F., Musso, P.-Y., Chan, R.C., Zhang, H.,
558 Feldman-Kiss, D., and Gordon, M.D. (2018). A complex peripheral code for
559 salt taste in Drosophila. Elife *7*, e37167.
560 12. Zhang, Y.V., Ni, J., and Montell, C. (2013). The molecular basis for attractive
561 salt-taste coding in Drosophila. Science *340*, 1334-1338.
562 13. Nakamura, M., Baldwin, D., Hannaford, S., Palka, J., and Montell, C. (2002).
563 Defective proboscis extension response (DPR), a member of the Ig
564 superfamily required for the gustatory response to salt. J. Neurosci. *22*, 3463-
565 3472.
566 14. Kim, H., Jeong, Y.T., Choi, M.S., Choi, J., Moon, S.J., and Kwon, J.Y. (2017).
567 Involvement of a *Gr2a*-Expressing *Drosophila* pharyngeal gustatory receptor
568 neuron in regulation of aversion to high-salt foods. Mol Cells *40*, 331-338.
569 10.14348/molcells.2017.0028.
570 15. Montell, C. (2021). *Drosophila* sensory receptors—a set of molecular Swiss
571 Army Knives. Genetics *217*, 1-34. 10.1093/genetics/iyaa011.
572 16. Ahn, J.-E., Chen, Y., and Amrein, H. (2017). Molecular basis of fatty acid taste
573 in Drosophila. Elife *6*, e30115.
574 17. Lee, Y., Poudel, S., Kim, Y., Thakur, D., and Montell, C. (2018). Calcium taste

575 avoidance in Drosophila. Neuron *97*, 67-74. e64.
576 18. Stanley, M., Ghosh, B., Weiss, Z.F., Christiaanse, J., and Gordon, M.D. (2021).
577 Mechanisms of lactic acid gustatory attraction in Drosophila. Current Biology
578 *31*, 3525-3537. e3526.
579 19. Shrestha, B., and Lee, Y. (2021). Mechanisms of carboxylic acid attraction in
580 Drosophila melanogaster. Molecules and Cells *44*, 900.
581 20. Rimal, S., Sang, J., Poudel, S., Thakur, D., Montell, C., and Lee, Y. (2019).
582 Mechanism of acetic acid gustatory repulsion in Drosophila. Cell reports *26*,
583 1432-1442. e1434.
584 21. Tauber, J.M., Brown, E.B., Li, Y., Yurgel, M.E., Masek, P., and Keene, A.C.
585 (2017). A subset of sweet-sensing neurons identified by IR56d are necessary
586 and sufficient for fatty acid taste. PLoS genetics *13*, e1007059.
587 22. Brown, E.B., Shah, K.D., Palermo, J., Dey, M., Dahanukar, A., and Keene,
588 A.C. (2021). Ir56d-dependent fatty acid responses in Drosophila uncover taste
589 discrimination between different classes of fatty acids. Elife *10*, e67878.
590 23. Kim, H., Kim, H., Kwon, J.Y., Seo, J.T., Shin, D.M., and Moon, S.J. (2018).
591 Drosophila Gr64e mediates fatty acid sensing via the phospholipase C
592 pathway. PLoS genetics *14*, e1007229.
593 24. Aryal, B., Dhakal, S., Shrestha, B., and Lee, Y. (2022). Molecular and
594 neuronal mechanisms for amino acid taste perception in the Drosophila
595 labellum. Current Biology *32*, 1376-1386. e1374.
596 25. Sánchez-Alcañiz, J.A., Silbering, A.F., Croset, V., Zappia, G.,
597 Sivasubramaniam, A.K., Abuin, L., Sahai, S.Y., Münch, D., Steck, K., and Auer,
598 T.O. (2018). An expression atlas of variant ionotropic glutamate receptors

599 identifies a molecular basis of carbonation sensing. Nature communications *9*,
600 4252.
601 26. Alves, G., Sallé, J., Chaudy, S., Dupas, S., and Manière, G. (2014). High-NaCl
602 perception in Drosophila melanogaster. Journal of Neuroscience *34*, 10884-
603 10891.
604 27. Liu, L., Leonard, A.S., Motto, D.G., Feller, M.A., Price, M.P., Johnson, W.A.,
605 and Welsh, M.J. (2003). Contribution of Drosophila DEG/ENaC genes to salt
606 taste. Neuron *39*, 133-146.
607 28. Chen, Y.D., and Dahanukar, A. (2017). Molecular and cellular organization of
608 taste neurons in adult *Drosophila* pharynx. Cell Rep. *21*, 2978-2991.
609 10.1016/j.celrep.2017.11.041.
610 29. Chen, Y.D., and Dahanukar, A. (2020). Recent advances in the genetic basis
611 of taste detection in *Drosophila*. Cell Mol Life Sci *77*, 1087-1101.
612 10.1007/s00018-019-03320-0.
613 30. Stocker, R.F. (1994). The organization of the chemosensory system in
614 *Drosophila melanogaster*: a review. Cell Tissue Res. *275*, 3-26.
615 31. Nayak, S.V., and Singh, R.N. (1983). Sensilla on the tarsal segments and
616 mouthparts of adult *Drosophila melanogaster* meigen (Diptera, Drosophilidae).
617 Int. J. Insect Morphol. Embryol. *12*, 273-291. Doi 10.1016/0020-
618 7322(83)90023-5.
619 32. LeDue, E.E., Chen, Y.C., Jung, A.Y., Dahanukar, A., and Gordon, M.D. (2015).
620 Pharyngeal sense organs drive robust sugar consumption in *Drosophila*. Nat.
621 Commun. *6*, 6667. 10.1038/ncomms7667.
622 33. Joseph, R.M., and Heberlein, U. (2012). Tissue-specific activation of a single

623 gustatory receptor produces opposing behavioral responses in Drosophila.
624 Genetics *192*, 521-532. 10.1534/genetics.112.142455.
625 34. Xiao, S., Baik, L.S., Shang, X., and Carlson, J.R. (2022). Meeting a threat of
626 the Anthropocene: Taste avoidance of metal ions by Drosophila. Proc Natl
627 Acad Sci U S A *119*, e2204238119. 10.1073/pnas.2204238119.
628 35. Soldano, A., Alpizar, Y.A., Boonen, B., Franco, L., Lopez-Requena, A., Liu, G.,
629 Mora, N., Yaksi, E., Voets, T., Vennekens, R., et al. (2016). Gustatory-
630 mediated avoidance of bacterial lipopolysaccharides via TRPA1 activation in
631 *Drosophila*. eLife *5*. 10.7554/eLife.13133.
632 36. Choi, J., van Giesen, L., Choi, M.S., Kang, K., Sprecher, S.G., and Kwon, J.Y.
633 (2016). A pair of pharyngeal gustatory receptor neurons regulates caffeine-
634 dependent ingestion in *Drosophila* larvae. Front Cell Neurosci *10*, 181.
635 10.3389/fncel.2016.00181.
636 37. Chen, Y.D., Menon, V., Joseph, R.M., and Dahanukar, A.A. (2021). Control of
637 sugar and amino acid feeding via pharyngeal taste neurons. J Neurosci *41*,
638 5791-5808. 10.1523/JNEUROSCI.1794-20.2021.
639 38. Joseph, R.M., Sun, J.S., Tam, E., and Carlson, J.R. (2017). A receptor and
640 neuron that activate a circuit limiting sucrose consumption. Elife *6*, e24992.
641 39. Marella, S., Fischler, W., Kong, P., Asgarian, S., Rueckert, E., and Scott, K.
642 (2006). Imaging taste responses in the fly brain reveals a functional map of
643 taste category and behavior. Neuron *49*, 285-295.
644 40. Klapoetke, N.C., Murata, Y., Kim, S.S., Pulver, S.R., Birdsey-Benson, A., Cho,
645 Y.K., Morimoto, T.K., Chuong, A.S., Carpenter, E.J., and Tian, Z. (2014).
646 Independent optical excitation of distinct neural populations. Nature methods

647 *11*, 338-346.
648 41. Nitabach, M.N., Blau, J., and Holmes, T.C. (2002). Electrical silencing of
649 Drosophila pacemaker neurons stops the free-running circadian clock. Cell
650 *109*, 485-495.
651 42. Dahanukar, A., Lei, Y.-T., Kwon, J.Y., and Carlson, J.R. (2007). Two Gr genes
652 underlie sugar reception in Drosophila. Neuron *56*, 503-516.
653 43. Thorne, N., Chromey, C., Bray, S., and Amrein, H. (2004). Taste perception
654 and coding in Drosophila. Current Biology *14*, 1065-1079.
655 44. Cameron, P., Hiroi, M., Ngai, J., and Scott, K. (2010). The molecular basis for
656 water taste in Drosophila. Nature *465*, 91-95.
657 45. Dambly-Chaudière, C., Jamet, E., Burri, M., Bopp, D., Basler, K., Hafen, E.,
658 Dumont, N., Spielmann, P., Ghysen, A., and Noll, M. (1992). The paired box
659 gene pox neuro: A determiant of poly-innervated sense organs in Drosophila.
660 Cell *69*, 159-172.
661 46. Aryal, B., Dhakal, S., Shrestha, B., Sang, J., Pradhan, R.N., and Lee, Y.
662 (2022). Protocol for binary food choice assays using Drosophila melanogaster.
663 STAR protocols *3*, 101410.
664 47. Sang, J., Dhakal, S., and Lee, Y. (2021). Cucurbitacin B suppresses
665 hyperglycemia associated with a high sugar diet and promotes sleep in
666 Drosophila melanogaster. Molecules and cells *44*, 68.
667 48. Chu, B., Chui, V., Mann, K., and Gordon, M.D. (2014). Presynaptic gain
668 control drives sweet and bitter taste integration in Drosophila. Current Biology
669 *24*, 1978-1984.
670 49. Benton, R., Vannice, K.S., Gomez-Diaz, C., and Vosshall, L.B. (2009). Variant

671 ionotropic glutamate receptors as chemosensory receptors in Drosophila. Cell
672 *136*, 149-162.
673 50. Thistle, R., Cameron, P., Ghorayshi, A., Dennison, L., and Scott, K. (2012).
674 Contact chemoreceptors mediate male-male repulsion and male-female
675 attraction during Drosophila courtship. Cell *149*, 1140-1151.
676 51. Gong, W.J., and Golic, K.G. (2003). Ends-out, or replacement, gene targeting
677 in Drosophila. Proceedings of the National Academy of Sciences *100*, 2556-
678 2561.
679 52. Lee, Y., Moon, S.J., and Montell, C. (2009). Multiple gustatory receptors
680 required for the caffeine response in Drosophila. Proceedings of the National
681 Academy of Sciences *106*, 4495-4500.
682 53. Lee, Y., Moon, S.J., Wang, Y., and Montell, C. (2015). A Drosophila gustatory
683 receptor required for strychnine sensation. Chemical senses *40*, 525-533.
684 54. Lee, Y., and Montell, C. (2013). Drosophila TRPA1 functions in temperature
685 control of circadian rhythm in pacemaker neurons. Journal of Neuroscience
686 *33*, 6716-6725.
687 55. Inagaki, H.K., Jung, Y., Hoopfer, E.D., Wong, A.M., Mishra, N., Lin, J.Y., Tsien,
688 R.Y., and Anderson, D.J. (2014). Optogenetic control of Drosophila using a
689 red-shifted channelrhodopsin reveals experience-dependent influences on
690 courtship. Nature methods *11*, 325-332.

691

692 # Figure legends

693 **Figure 1. Requirements for four *Ir*s for preferred high salt-containing food and**
694 **chemogenetic and optogenetic control of *Ir60b*-positive GRNs**

695 (A) Binary food choice assay comparing 30 *Ir*-mutants to the control strain (w^{1118}) for
696 high salt avoidance, n=8–12.

697 (B) Preference of indicated flies observed at various concentrations of NaCl, n=8–12.

698 (C) The gustatory response to the activation of *Gr64f* GRNs or *Ir60b* GRNs by
699 feeding capsaicin to *trpV1*-expressing flies was tested. Binary food choice assays
700 were performed with the indicated flies. The presence or absence of the transgene is
701 indicated by "+" and "-", respectively. n=8.

702 (D) Optogenetics was employed to measure PER in the indicated flies using red light
703 and sucrose stimulation at the same time. n=6.

704 Multiple sets of data were compared using single-factor ANOVA coupled with
705 Scheffe's post hoc test. Statistical significance compared with the control was
706 denoted by asterisks (**$p < 0.01$). All error bars represent the standard error of the
707 mean (SEM).

708

709 **Figure 2. The requirement of pharyngeal *Ir60b*-GRNs in high salt avoidance**

710 (A) Schematic representation illustrating the gustatory sensilla arrangement on the
711 fly labellum, following Tanimura's nomenclature.

712 (B) Tip recording analyses conducted on S4, S8, and L4 sensilla using control,
713 *Ir7c*^{GAL4}, *Ir25a*^{2}, *Ir60b*^{3}, and *Ir76b*^{1} strains at 300 mM NaCl, n=10–16.

714 (C) Representative sample traces obtained from S4 sensillum in (D).

715 (D) Binary food choice assays comparing specific GRN-ablated flies to the control
716 strain, with each genotype indicated by different colors. n=12.

717 (E) Tip recording analyses conducted on S4 and S8 sensilla using specific GRN-
718 ablated flies and the control strain at 300 mM NaCl, with each genotype indicated by
719 different colors. n=16–20.

720 (F-I) Proboscis extension reflex (PER) assay was performed using *Ir25a*^{2}, *Ir60b*^{3},
721 *Ir76b*^{1}, and control strain, n=8–10.

722 (F) PER percentages induced by first 2% sucrose.

723 (G) PER percentages induced by first 2% sucrose with 300 mM NaCl.

724 (H) PER percentages induced by secondary 2% sucrose.

725 (I) PER percentages is induced by secondary 2% sucrose with 300 mM NaCl.

726 (J) Binary food choice assays for 300 mM salt avoidance were conducted with *Poxn*
727 mutant (*Poxn*$^{70\text{-}28}$/*Poxn*$^{\Delta M22\text{-}B5}$), *Ir25a*^{2}, *Ir60b*^{3}, *Ir76b*^{1}, double mutant (*Poxn*$^{70\text{-}}$
728 ^{28}/*Poxn*$^{\Delta M22\text{-}B5}$;*Ir60b*^{3}), and control strain, n=9–12.

729 All error bars represent SEM. Multiple sets of data were compared using single-
730 factor ANOVA coupled with Scheffe's post hoc test. Statistical significance compared
731 with the controls or the *Poxn*$^{70\text{-}28}$/*Poxn*$^{\Delta M22\text{-}B5}$ is denoted by black or red asterisks,
732 respectively (**$p < 0.01$).

733

734 **Figure 3. Measurement of food intake utilizing the DrosoX system**

735 (A-P) The figures present the ingestion amounts (A, C, E, G, I, K, M and O) and the
736 ingestion index (B, D, F, H, I, J, L, N and P).

737 (A-N) The ingestion of (a)100 mM sucrose alone and (b) in combination with 300 mM
738 NaCl was determined using the Droso-X assay.

739 (A and B) Measurement of food intake with control, *Ir25a*^{2}, *Ir60b*^{3}, and *Ir76b*^{1}, n=12.

740 (C and D) Genetically recovered flies of *Ir60b*^{3} driven by *Ir60b-GAL4*, n=12.

741 (E and F) Genetically recovered flies of *Ir25a*^{2} driven by *Ir25a-GAL4*, n=12.

742 (G and H) Genetically recovered flies of *Ir76b*^{1} driven by *Ir76b-GAL4*, n=12.

743 (I and J) Genetically recovered flies of *Ir25a*^{2} driven by *Ir60b-GAL4*, n=12.

744 (K and L) Genetically recovered flies of *Ir76b*^{1} driven by *Ir60b-GAL4*, n=12.

745 (M and N) Genetically recovered flies of *Ir60b*^{3} driven by *Ir25a-GAL4* and *Ir76b-*
746 *GAL4* respectively, n=12.

747 (O and P) Measurement of food intake with control, *Ir60b*^{3}, and *Gr66a*^{ex83} at 100 mM
748 sucrose versus 100 mM sucrose with 10 mM caffeine, n=12.

749 All error bars represent SEM. Multiple sets of data were compared using single-
750 factor ANOVA coupled with Scheffe's post hoc test. Statistical significance compared
751 with the controls (A and P) or each *UAS* only in the mutant condition (D, F, H, J, L
752 and N), is denoted by color asterisks (**$p < 0.01$).

753

754 **Figure 4. Immunohistochemistry and calcium imaging experiments in the**

755 **IR60b GRNs**

756 (A) Immunohistochemistry was performed using anti-GFP and anti-RFP to visualize

757 the LSO in the pharynx of *UAS-mCD8*::*GFP*/*Ir76b-QF2*;*Ir60b-GAL4*/*QUAS-tdTomato*.

758 (B) Immunohistochemistry was conducted using anti-GFP and anti-RFP to visualize

759 the LSO in the pharynx of *Ir25a-GAL4*/*Ir76b-QF2*;*UAS-mCD8*::*GFP*/*QUAS-tdTomato*.

760 (C) Heat map images illustrate changes in GCaMP6f fluorescence before and after

761 stimulation with 300 mM NaCl using the indicated flies.

762 (D) Sample traces depict the responses of *UAS-GCaMP6f*;*Ir60b-GAL4* to 300 mM

763 NaCl with $Ir25a^2$, $Ir60b^3$, $Ir76b^1$, and control strains. n=10–14.

764 (E) Quantification of *UAS-GCaMP6f*;*Ir60b-GAL4* responses to various

765 concentrations of NaCl on control, $Ir25a^2$, $Ir60b^3$, and $Ir76b^1$, respectively, n=10–14.

766 (F) Quantification of GCaMP6f responses to 300 mM NaCl on the indicated mutants

767 and rescued flies, n=8–10. The presence or absence of the transgene is indicated by

768 "+" and "-", respectively.

769 (G) Quantification of *UAS-GCaMP6f*;*Ir60b-GAL4* responses to 50 mM, 300 mM, and

770 500 mM of $CaCl_2$, $MgCl_2$, and KCl on control, n=10–14.

771 (H) Quantification of *UAS-GCaMP6f*;*Ir60b-GAL4* responses to various

772 concentrations of NaBr on control, $Ir25a^2$, $Ir60b^3$, and $Ir76b^1$, respectively, n=10–14.

773 (I) Quantification of *UAS-GCaMP6f*;*Ir60b-GAL4* responses to 5 mM and 50 mM

774 concentrations of bitter compounds (quinine, caffeine, strychnine, lobeline,

775 denatonium, and coumarin), n=8–10.

776 (J) Quantification of *UAS-GCaMP6f;Ir60b-GAL4* responses to various concentrations

777 of sucrose on control, *Ir25a*^{2}, *Ir60b*^{3}, and *Ir76b*^{1}, respectively, n=10–14.All error bars

778 represent the SEM. Multiple sets of data were compared using single-factor ANOVA

779 coupled with Scheffe's post hoc test. Statistical significance compared with the

780 controls is indicated by asterisks (**$p < 0.01$).

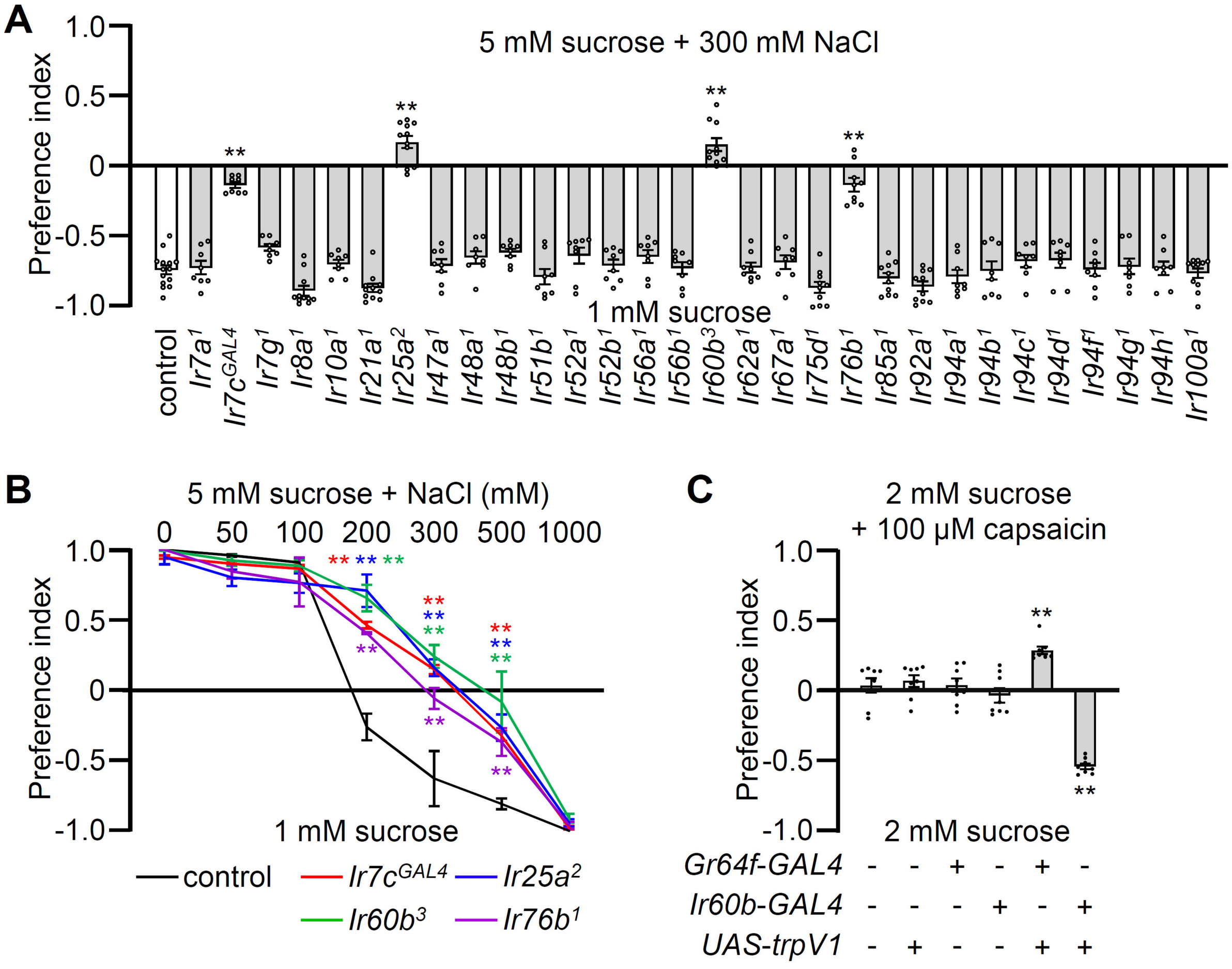
A
5 mM sucrose + 300 mM NaCl
Preference index
1.0
0.5
0
-0.5
-1.0
1 mM sucrose
control
Ir7a1
Ir7cGAL4
Ir7g1
Ir8a1
Ir10a1
Ir21a1
Ir25a2
Ir47a1
Ir48a1
Ir48b1
Ir51b1
Ir52a1
Ir52b1
Ir56a1
Ir56b1
Ir60b3
Ir62a1
Ir67a1
Ir75d1
Ir76b1
Ir85a1
Ir92a1
Ir94a1
Ir94b1
Ir94c1
Ir94d1
Ir94f1
Ir94g1
Ir94h1
Ir100a1
B
5 mM sucrose + NaCl (mM)
0 50 100 200 300 500 1000
Preference index
1 mM sucrose
control
Ir7cGAL4
Ir25a2
Ir60b3
Ir76b1
C
2 mM sucrose
+ 100 μM capsaicin
Preference index
2 mM sucrose
Gr64f-GAL4 - - + - + -
Ir60b-GAL4 - - - + - +
UAS-trpV1 - + - - + +
D
PER (%)
+>CsChrimson
Gr5a>CsChrimson
Gr66a>CsChrimson
Ir60b>CsChrimson

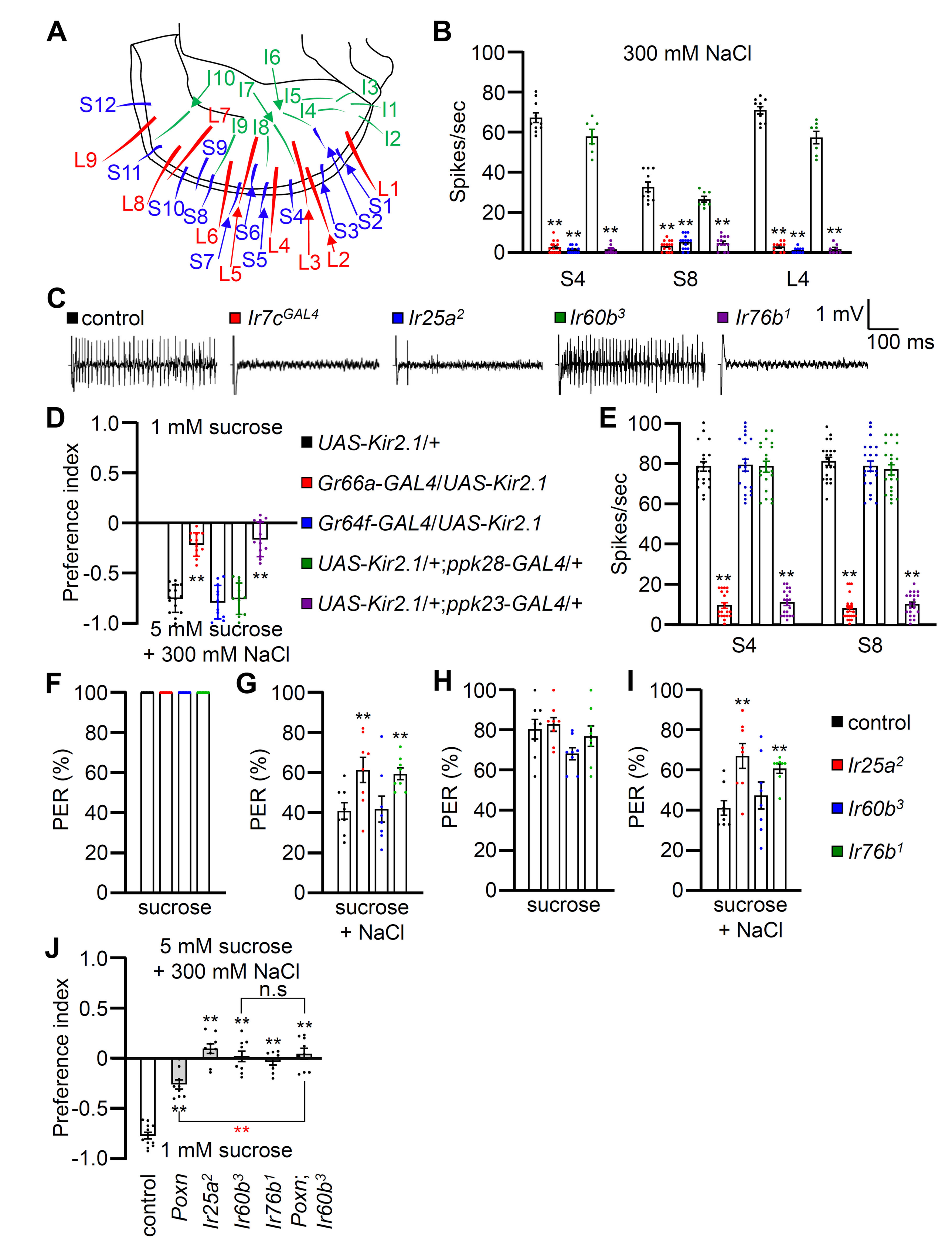
A
S12
L9
S11
L8
S10
S8
S9
L7
L6
S7
S6
L5
S5
L4
S4
L3
L2
S3
S2
L1
S1
I10
I7
I9
I8
I6
I5
I4
I3
I1
I2
B
300 mM NaCl
Spikes/sec
S4
S8
L4
C
control
Ir7c^GAL4
Ir25a^2
Ir60b^3
Ir76b^1
1 mV
100 ms
D
1 mM sucrose
5 mM sucrose
+ 300 mM NaCl
Preference index
UAS-Kir2.1/+
Gr66a-GAL4/UAS-Kir2.1
Gr64f-GAL4/UAS-Kir2.1
UAS-Kir2.1/+;ppk28-GAL4/+
UAS-Kir2.1/+;ppk23-GAL4/+
E
Spikes/sec
S4
S8
F
PER (%)
sucrose
G
PER (%)
sucrose
+ NaCl
H
PER (%)
sucrose
I
PER (%)
sucrose
+ NaCl
control
Ir25a^2
Ir60b^3
Ir76b^1
J
5 mM sucrose
+ 300 mM NaCl
n.s
Preference index
1 mM sucrose
control
Poxn
Ir25a^2
Ir60b^3
Ir76b^1
Poxn;
Ir60b^3

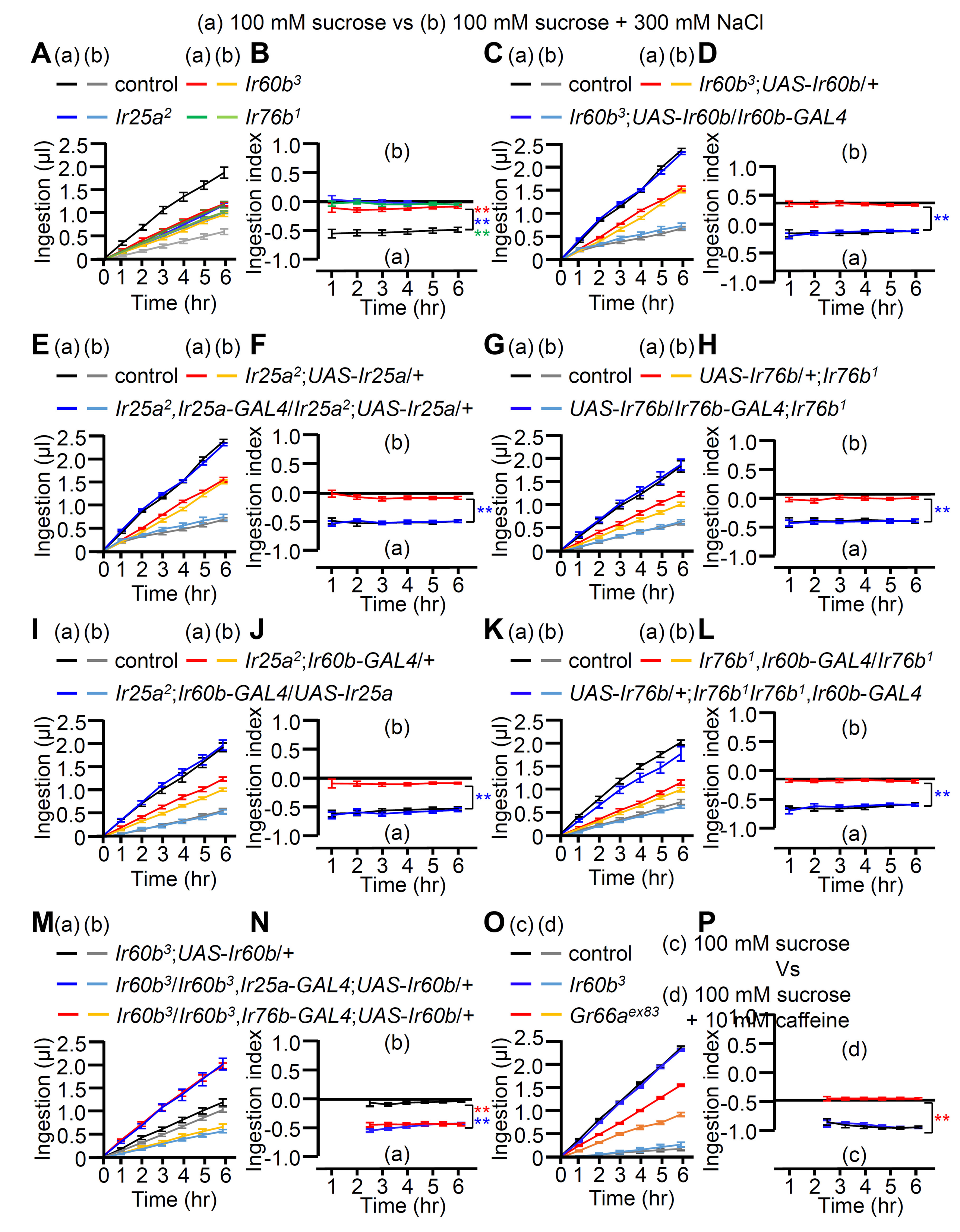
(a) 100 mM sucrose vs (b) 100 mM sucrose + 300 mM NaCl
A
B
C
D
control
Ir60b3
Ir25a2
Ir76b1
Ir60b3;UAS-Ir60b/+
Ir60b3;UAS-Ir60b/Ir60b-GAL4
E
F
G
H
Ir25a2;UAS-Ir25a/+
Ir25a2,Ir25a-GAL4/Ir25a2;UAS-Ir25a/+
UAS-Ir76b/+;Ir76b1
UAS-Ir76b/Ir76b-GAL4;Ir76b1
I
J
K
L
Ir25a2;Ir60b-GAL4/+
Ir25a2;Ir60b-GAL4/UAS-Ir25a
Ir76b1,Ir60b-GAL4/Ir76b1
UAS-Ir76b/+;Ir76b1Ir76b1,Ir60b-GAL4
M
N
O
P
Ir60b3;UAS-Ir60b/+
Ir60b3/Ir60b3,Ir25a-GAL4;UAS-Ir60b/+
Ir60b3/Ir60b3,Ir76b-GAL4;UAS-Ir60b/+
Gr66aex83
(c) 100 mM sucrose
Vs
(d) 100 mM sucrose
+ 10 mM caffeine
Ingestion (µl)
Ingestion index
Time (hr)
**

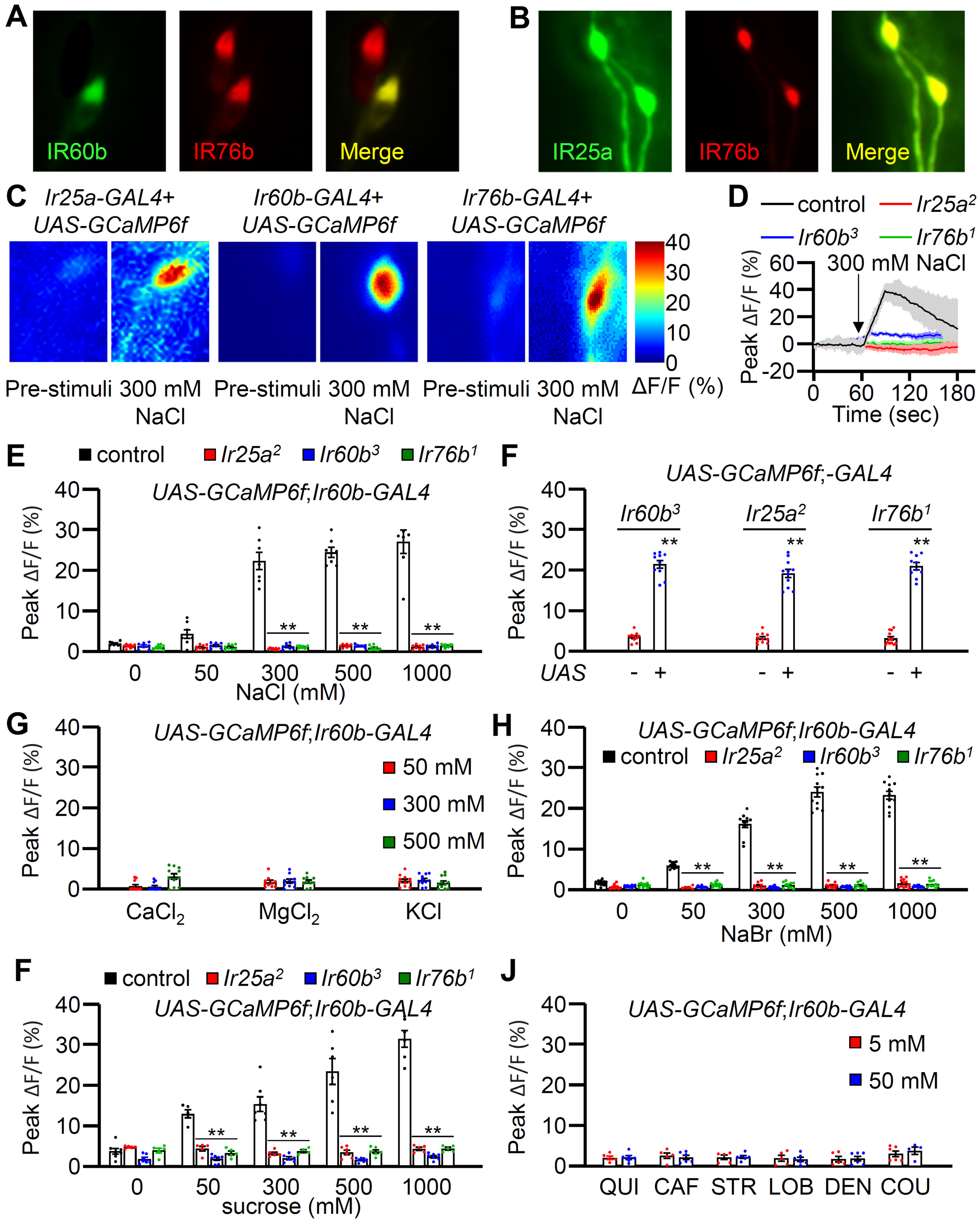
A
IR60b
IR76b
Merge
B
IR25a
IR76b
Merge
C
Ir25a-GAL4+ UAS-GCaMP6f
Ir60b-GAL4+ UAS-GCaMP6f
Ir76b-GAL4+ UAS-GCaMP6f
Pre-stimuli 300 mM NaCl
Pre-stimuli 300 mM NaCl
Pre-stimuli 300 mM NaCl
ΔF/F (%)
D
control
Ir25a2
Ir60b3
Ir76b1
300 mM NaCl
Peak ΔF/F (%)
Time (sec)
E
control
Ir25a2
Ir60b3
Ir76b1
UAS-GCaMP6f;Ir60b-GAL4
Peak ΔF/F (%)
NaCl (mM)
F
UAS-GCaMP6f;-GAL4
Ir60b3
Ir25a2
Ir76b1
Peak ΔF/F (%)
UAS
G
UAS-GCaMP6f;Ir60b-GAL4
50 mM
300 mM
500 mM
Peak ΔF/F (%)
CaCl2
MgCl2
KCl
H
UAS-GCaMP6f;Ir60b-GAL4
control
Ir25a2
Ir60b3
Ir76b1
Peak ΔF/F (%)
NaBr (mM)
F
control
Ir25a2
Ir60b3
Ir76b1
UAS-GCaMP6f;Ir60b-GAL4
Peak ΔF/F (%)
sucrose (mM)
J
UAS-GCaMP6f;Ir60b-GAL4
5 mM
50 mM
Peak ΔF/F (%)
QUI
CAF
STR
LOB
DEN
COU